ISSN 1674-1056
http://cpb.iphy.ac.cn
http://iopscience.iop.org/cpb
中国物理 B
Chinese Physics
中国物理 Chinese Physics B

Simulation of SiC radiation detector degradation

Hai-Li Huang(黄海栗), Xiao-Yan Tang(汤晓燕), Hui Guo(郭辉), Yi-Men Zhang(张义门), Yu-Tian Wang(王雨田), Yu-Ming Zhang(张玉明)

Citation: Chin. Phys. B . 2019, 28(1): 010701. **doi:** 10.1088/1674-1056/28/1/010701
Journal homepage: http://cpb.iphy.ac.cn; http://iopscience.iop.org/cpb

What follows is a list of articles you may be interested in

Effect of different bending shapes on thermal properties of flexible light-emitting diode filament

Liping Wang(王立平), Wenbo Li(李文博), Yichao Xu(徐一超), Bobo Yang(杨波波), Mingming Shi(石明明), Jun Zou(邹军), Yang Li(李杨), Xinglu Qian(钱幸璐), Fei Zheng(郑飞), Lei Yang(杨磊)

Chin. Phys. B . 2018, 27(11): 110701. **doi:** 10.1088/1674-1056/27/11/110701

A rapid and convenient experimental method of absolutely calibrating transmission of x-ray flat-response filter

Jian Yu(余建), Li-Fei Hou(候立飞), Jing Wang(王静), Wen-Hai Zhang(张文海), Ming Chen(陈铭), Bao-Chong Zhou(周保充), Sha-Li Xiao(肖沙里), Shen-Ye Liu(刘慎业)

Chin. Phys. B . 2018, 27(10): 100702. **doi:** 10.1088/1674-1056/27/10/100702

Baseline optimization for scalar magnetometer array and its application in magnetic target localization

Li-Ming Fan(樊黎明), Quan Zheng(郑权), Xi-Yuan Kang(康曦元), Xiao-Jun Zhang(张晓峻), Chong Kang(康崇)

Chin. Phys. B . 2018, 27(6): 060703. **doi:** 10.1088/1674-1056/27/6/060703

Nested grazing incidence optics for x ray detection

Lin-Sen Li(李林森), Peng-Fei Qiang(强鹏飞), Li-Zhi Sheng(盛立志), Yong-An Liu(刘永安), Zhe Liu(刘哲), Duo Liu(刘舵), Bao-Sheng Zhao(赵宝升), Chun-Min Zhang(张淳民)

Chin. Phys. B . 2017, 26(10): 100703. **doi:** 10.1088/1674-1056/26/10/100703

Effective transport of passive particles induced by chiral-active particles in microchannel

Yunfeng Hua(华昀峰), Linli He(何林李), Linxi Zhang(章林溪)

Chin. Phys. B . 2017, 26(8): 080702. **doi:** 10.1088/1674-1056/26/8/080702

Simulation of SiC radiation detector degradation*

Hai-Li Huang(黄海栗)[1,2], Xiao-Yan Tang(汤晓燕)[1,2,†], Hui Guo(郭辉)[1,2], Yi-Men Zhang(张义门)[1,2], Yu-Tian Wang(王雨田)[1,2], and Yu-Ming Zhang(张玉明)[1,2]

[1] *School of Microelectronics, Xidian University, Xi'an* 710071, *China*

[2] *Key Laboratory of Wide Band-Gap Semiconductor Materials and Devices, Xidian University, Xi'an* 710071, *China*

(Received 20 September 2018; revised manuscript received 30 October 2018; published online 12 December 2018)

Simulation on the degradation of 4H-SiC Schottky detector was carried out using ISE TCAD, and the limit of the drift-diffusion analytical model was discussed. Two independent defect levels, rather than a pair of specific carrier lifetime, were induced to describe $Z1/2$ defects in simulation to calculate the charge collection efficiency versus bias voltage. Comparison between our calculation and the reported experimental results shows that an acceptable agreement was achieved, proving the feasibility of regarding $Z1/2$ defect as two individual defect levels. Such a treatment can simplify the simulation and may help to further investigate the detector degradation.

Keywords: 4H-SiC, detector degradation, simulation, $Z1/2$ defect

PACS: 07.85.Fv, 29.85.Fj, 29.40.–n **DOI:** 10.1088/1674-1056/28/1/010701

1. Introduction

Silicon carbide (SiC) as the third generation semiconductor has many outstanding properties, such as wide bandgap, high critical electric field strength, large carrier saturation velocity, high thermal conductivity, and good radiation resistance, which make it suitable for radiation detectors working in high temperature and high radiation conditions.[1,2] SiC based radiation detectors are presently being developed for applications in the energetic particle detection, such as α, β, x-ray, and neutron, which would deteriorate the performance of devices.[3–5]

To quantitatively characterize the degradation of a detector, minority carrier lifetime, defect concentration, and effective doping concentration ($N_{\rm eff}$) are commonly extracted before and after irradiation. But either trap induction rate or doping compensation rate varies with the type and energy of the incident particle, and the defect affecting the minority carrier lifetime, namely $Z1/2$ defect, is not a single energy level defect,[6–8] leaves it a challenge to predict the degradation of carrier lifetime, thus the degradation of a detector. Quinn *et al*. investigated detector degradation by using defect models in MEDICI simulations. A relative simple $Z1/2$ model including single energy defect level with one cross-section was investigated without providing the comparison between simulation and experimental results.

In this paper, detector performance is simulated by ISE-TCAD, comparing with the degradation results reported in Ref. [9]. A different approach inducing $Z1/2$ defect as two individual defect energy levels, instead of modifying carrier lifetime of SiC, is adopted in our simulation. Acceptable agreement is achieved by comparing the simulated charge collection efficiency (CCE) with the reported one. It shows that the presented model to deal with $Z1/2$ defect is applicable for degradation analysis. Based on the approach mentioned above, this work focuses on building a scheme to further predict the degradation of detector performance during its operation.

2. Minority carrier lifetime and defect concentration

In Ref. [9], the doping compensation and carrier lifetime reduction were considered as the main factors that lead to the degradation. $N_{\rm eff}$ was calculated through C–V measurement and carrier lifetime was extracted from the variation of CCE with bias voltage. Theoretical CCE versus bias voltage is typically obtained by drift-diffusion analytical expression[10,11]

$$\mathrm{CCE} = \frac{1}{N_{\rm n,p}}\int_0^{x_{\rm d}} G(x)\,{\rm d}x + \frac{1}{N_{\rm n,p}}\int_{x_{\rm d}}^{R_{\rm dep}} G(x)\exp\left(-\frac{x-x_{\rm d}}{L_{\rm p}}\right){\rm d}x, \quad (1)$$

where $N_{\rm n,p}$ is the total amount of generated electron–hole pairs (e–h), $x_{\rm d}$ is the depletion layer width at a bias voltage, $R_{\rm dep}$ is the penetration depth of ions, $G(x)$ is the e–h generation profile, and $L_{\rm p}$ is the hole diffusion length.

As $L_{\rm p}$ is a function of hole lifetime ($\tau_{\rm p}$), CCE is a function of $\tau_{\rm p}$ if the working condition of the device and the incident particle are given. A constant value of $\tau_{\rm p}$ is given by the Shockley–Read–Hall (SRH) theorem[12]

$$\tau_{\rm p} = \frac{1}{a_{\rm p}N_{\rm t}}, \quad (2)$$

where $N_{\rm t}$ is the defect concentration and $a_{\rm p}$ is the hole capture coefficient. But such a $\tau_{\rm p}$ could only be an equivalent

*Project supported by the National Key R&D Program of China (Grant No. 2016YFB0400400).

†Corresponding author. E-mail: xytang@mail.xidian.edu.cn

© 2019 Chinese Physical Society and IOP Publishing Ltd http://iopscience.iop.org/cpbIOP161ZIOP161Z http://cpb.iphy.ac.cn

value, because equation (2) is subjected to a precondition that the equilibrium electron density, which is approximate to net doping concentration N_d, is much larger than the excess hole density δp.

Figure 1 shows the simulation result of a 2 MeV α particle perpendicular incidence into a SiC schottky detector at a bias voltage of -10 V. The integrated charge of such a current pulse reaches 90% of its maximum at time 3.22 ns after the bombardment. The profiles of electron density and hole density at different moments after the bombardment are plotted in Fig. 1(b). Obviously, the condition of $N_d \gg \delta p$ is not satisfied even if 4 ns has passed.

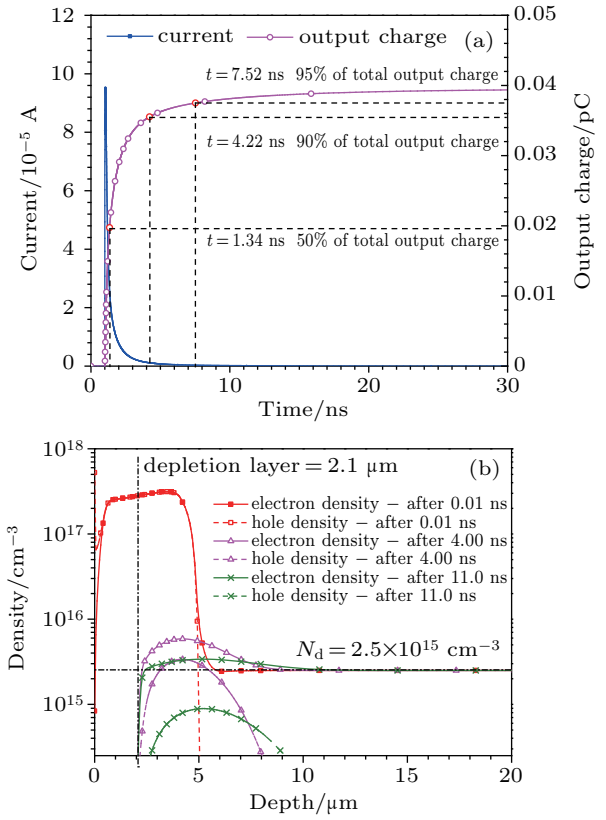


Fig. 1. Incidence of a 2 MeV α particle into a -10 V biased SiC Schottky detector at 1 ns: (a) pulse current and integrated output charge, (b) electron and hole density along the trajectory at different moments.

In addition, for the condition $\delta n \approx \delta p \gg N_d$, namely the high injection condition, the recombination rate R could be written as

$$R = \frac{\delta p}{\tau_p + \tau_n}, \tag{3}$$

where τ_n is defined as the electron lifetime, and given as

$$\tau_n = \frac{1}{a_n N_t}, \tag{4}$$

a_n is the electron capture coefficient of the defect level.

Thus, it is improper to use the extracted τ_p from Eq. (1) in TCAD simulation, and τ_n also has an effect on the CCE calculation, which will be discussed later.

Considering the fact that a decreasing τ_p results from an increasing N_t, which is the concentration of $Z1/2$ defect in this case, it is preferred to induce defect levels when calculating current pulses. It should be noted that, N_t can be obtained neither from Eq. (2) nor from Eq. (3) using a τ_p extracted from Eq. (1).

3. Setting parameters

A schematic cross-section of detectors reported in Ref. [9] is shown in Fig. 2. Values of N_{eff}, Schottky barrier height φ_b, and ideal factor n before and after radiation are listed in Table 1.

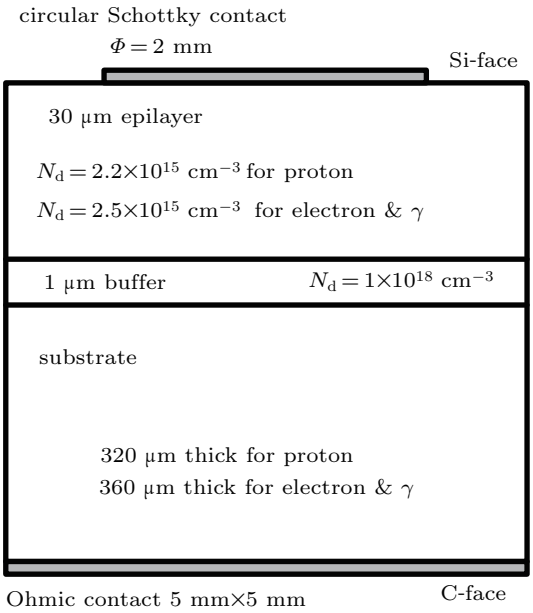


Fig. 2. Schematic cross-section of detectors reported in Ref. [9].

Table 1. Detector parameters before and after irradiation reported in Ref. [9].

Irradiation	Dose	N_{eff}/cm^{-3}	φ_b/eV	n
24 GeV proton	unirradiated	2.18×10^{15}	1.70	1.19
24 GeV proton	9.37×10^{13} cm^{-2}	1.43×10^{15}	1.72	1.18
8.2 MeV electron	unirradiated	2.49×10^{15}	1.03	1.034
8.2 MeV electron	20 Mrad	1.67×10^{15}	1.13	1.036
8.2 MeV electron	40 Mrad	6.89×10^{14}	1.54	1.032
^{60}Co γ		2.49×10^{15}	1.03	1.034
^{60}Co γ	20 Mrad	2.28×10^{15}	1.03	1.033
^{60}Co γ	40 Mrad	2.21×10^{15}	1.03	1.034

To find out N_t in the electron irradiated device, energy deposition in a 390 μm thick SiC layer by 8.2 MeV electron is carried out by CASINO 2.4. As shown in Fig. 3, the distribution of energy deposition is uniform, and nearly 99% of the transmitted electrons remain at an energy of 7.95 MeV. Thus, a dose of 40 Mrad is equivalent to a fluence of 1.33×10^{15} cm^{-2}. As the $Z1/2$ defect introduction rate of 8.2 MeV electron is 0.44–0.57 cm^{-1} reported in Ref. [13], N_t is obtained as 5.89–7.63×10^{14} cm^{-3}.

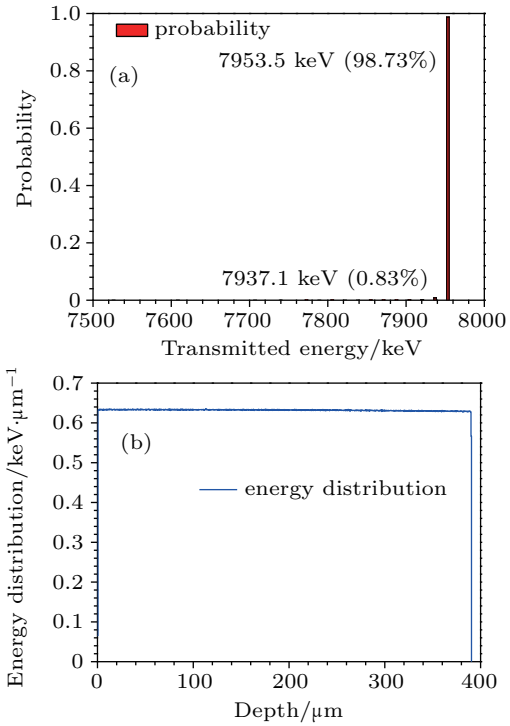


Fig. 3. Simulation result from CASINO 2.4. Vertical incidence of 8.2 MeV electrons into a 390 μm SiC layer. (a) Energy of the transmitted electrons. (b) Profile of energy deposition in SiC.

A defect introduction rate of 24 GeV protons has never been reported. Considering that both a 24 GeV proton and 8.2 MeV electron will pass through a 390 μm thick SiC layer easily, and τ_p extracted for the proton irradiated (9.37×10^{13} cm^{-2}) device is 3.3 ns and is almost the same as that of the 40 Mrad electron irradiated device. Thus, it may be assumed that N_t of the proton irradiated device is approximate to that of the electron irradiated device, and both N_t are evenly distributed.

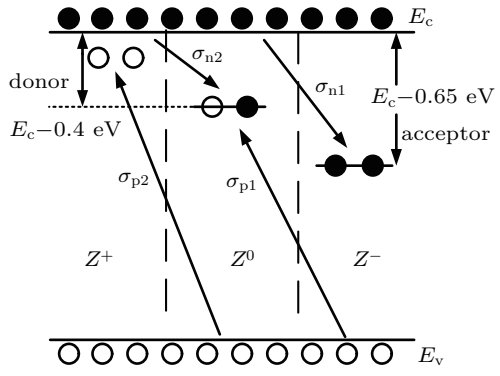


Fig. 4. Schematic of carrier capture and emission at the $Z1/2$ defect.

The $Z1/2$ defect can trap two electrons and thus has three charge states, i.e., empty (Z^+), singly occupied (Z^0), and doubly occupied (Z^-) states. Figure 4 shows the schematic of free carrier capture and emission at $Z1/2$ defect. Transitions between Z^- and Z^0 and between Z^0 and Z^+ are measured as an acceptor state at $E_c-0.65$ eV and a donor state at $E_c-0.4$ eV, respectively; $\sigma_{n1}(\sigma_{n2})$ and $\sigma_{p1}(\sigma_{p2})$ stand for the electron and hole capture cross sections of the acceptor (donor) state. Parameters of $Z1/2$ are listed in Table 2, including the defect energy levels, charge states, and carrier capture cross-sections.

Table 2. Parameters of $Z1/2$ defect at 300 K from Ref. [8].

Energy level	Type	Electron capture cross-section/cm^2	Hole capture cross-section/cm^2
$E_c-0.40$/eV	donor	5.494×10^{-15}	1.986×10^{-14}
$E_c-0.65$/eV	acceptor	0.945×10^{-16}	1.1×10^{-13}

Although the donor level and the acceptor level interact with each other, they can be treated as two independent levels and both two-interacted-levels model and two-independent-levels model will lead to the same carrier lifetime if the following conditions are satisfied:[14]

$$\begin{cases} \exp\left(\dfrac{\delta E}{kT}\right) \gg \dfrac{\sigma_{n2}}{\sigma_{n1}},\ \dfrac{\sigma_{p1}}{\sigma_{p2}}, \\ \dfrac{\sigma_{n2}}{\sigma_{n1}},\ \dfrac{\sigma_{p1}}{\sigma_{p2}} \gg 1, \end{cases} \tag{5}$$

where δE is the gap between the donor state and acceptor state, and equals 0.25 eV in our case; k is the Boltzmann constant, and T is the temperature in Kelvin. Only the condition of $\sigma_{p1}/\sigma_{p2}\gg1$ is not well satisfied. Thus, we may induce the two-independent-levels model in our simulation.

In addition, CCE is considered as 1 when unirradiated SiC Schottky detectors are biased −1000 V. In this case, the thickness of the depletion layer reaches 22 μm. As the penetration depth is about 18 μm for a 5.486 MeV α particle in SiC, the excited e–h pairs by the injected high energy particles are completely laid in the space charge region.

4. Simulation results and discussion

CCE versus applied voltage was calculated based on several basic parameter models, such as (i) SRH and Auger recombination models, (ii) high field saturation and carrier–carrier scattering mobility models, and (iii) trap models.[15] CCE_{sim} and CCE_{exp} hereafter stand for the calculated CCE and the reported experimental CCE in Ref. [9], respectively.

In addition, except for the case which would add no trap and modify the carrier lifetime directly, τ_n and τ_p are set as 0.6 μs and 0.3 μs respectively to ensure the agreement between CCE_{sim} and CCE_{exp} for diodes before irradiation (see Fig. 9, $N_t=0$).

4.1. CCE calculated with specific τ_n and τ_p

Figure 5 shows the effect of τ_n on CCE when τ_p remains a same value of 3 ns as Ref. [9]; CCE decreases with decreasing τ_n for a fixed applied voltage. As can be seen from this figure, CCE_{sim} well agrees with CCE_{exp} only if τ_n is equal to or smaller than 1 ns.

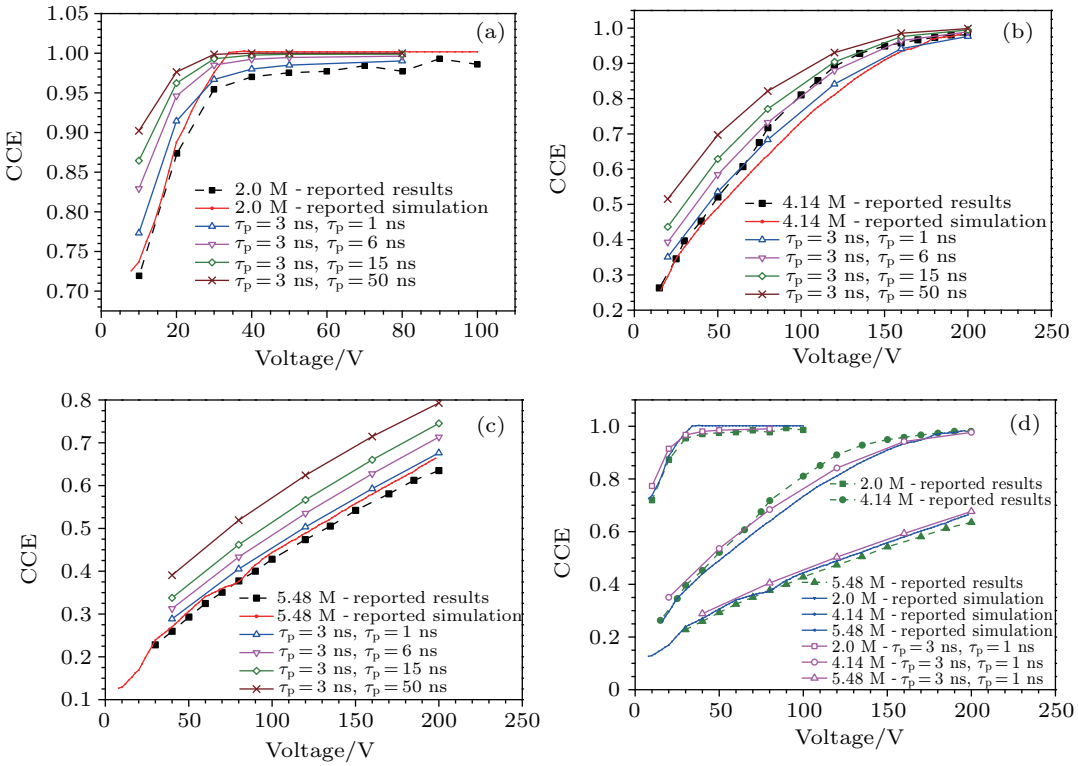


Fig. 5. Comparison between CCE_{exp} and CCE_{sim} obtained with different τ_n. (a) CCE_{sim} for 2.0 MeV α particle, (b) CCE_{sim} for 4.14 MeV α particle, (c) CCE_{sim} for 5.48 MeV α particle, (d) CCE_{sim} when $\tau_n = 1$ ns and $\tau_p = 3$ ns.

4.2. Proton irradiated detector

Considering that the defect density in the proton irradiated device is assumed to have the same value as that in the 40 Mrad electron irradiated device, N_t in the proton irradiated detector can be taken as 5.89–7.63 $\times$ 10^{14} cm^{-3}. Thus, three values of N_t (5.89 $\times$ 10^{14} cm^{-3}, 6.76 $\times$ 10^{14} cm^{-3}, and 7.63 $\times$ 10^{14} cm^{-3}) were adopted to find out the optimum N_t value. To make a comparison, an additional $N_t = 4.2 \times 10^{14}$ cm^{-3}, refered to $\tau_p = 3$ ns as calculated from Eq. (2), was also adopted. The results are plotted in Fig. 6.

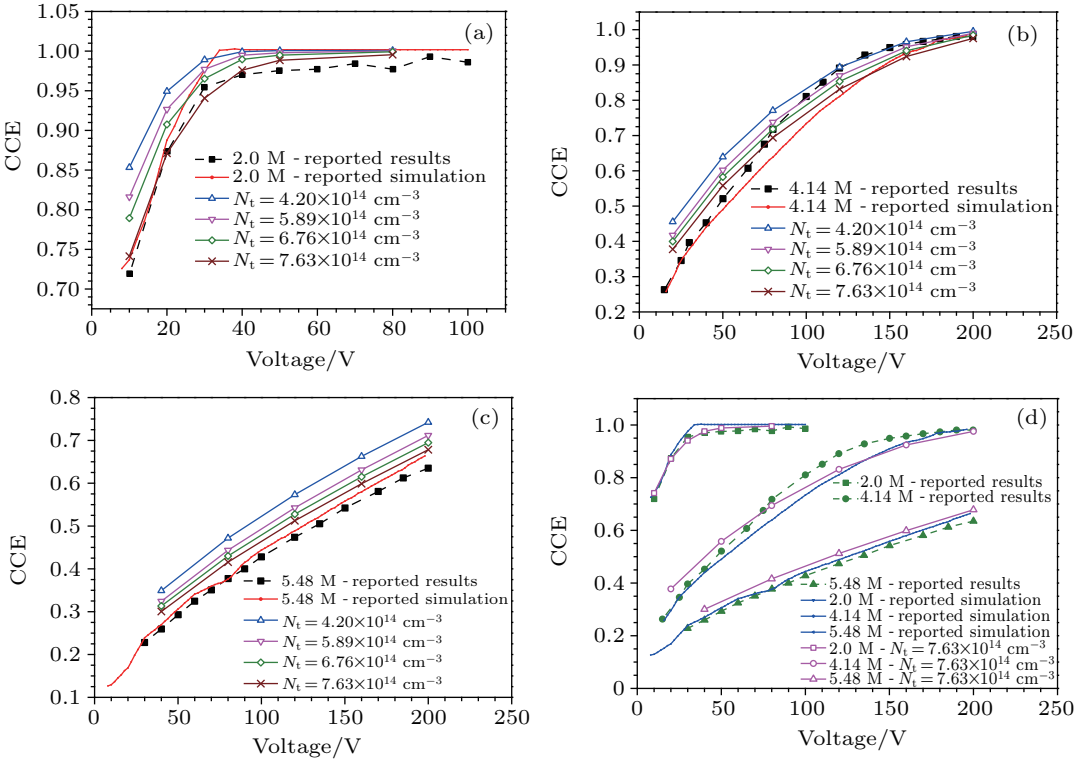


Fig. 6. Comparison between CCE_{exp} and CCE_{sim} obtained with different N_t for proton irradiated detector. (a) CCE_{sim} for 2.0 MeV α particle, (b) CCE_{sim} for 4.14 MeV α particle, (c) CCE_{sim} for 5.48 MeV α particle, (d) CCE_{sim} when $N_t = 7.63 \times 10^{14}$ cm^{-3}.

Among these four N_t values, CCE obtained with $N_t = 7.63 \times 10^{14}$ cm^{-3} shows the best agreement. In case of 2 MeV α particles, CCE_{sim} is almost the same as CCE_{exp}. For the 5.48 MeV α particles irradiation case, CCE_{sim} is similar to CCE_{exp}, a small difference of about 0.04 is observed. CCE_{sim} of 4.14 MeV α shows a relative poor agreement compared with the other two cases, especially for the voltage between 100 V and 150 V. As reported in Ref. [9], their simulation result had a similar trend. It is suggested that the 4.14 MeV α particles might actually have their own uncertainty of energies when they reached the surface of the detector, as such energy was obtained by decelerating the ^{241}Am α-radiation in air.

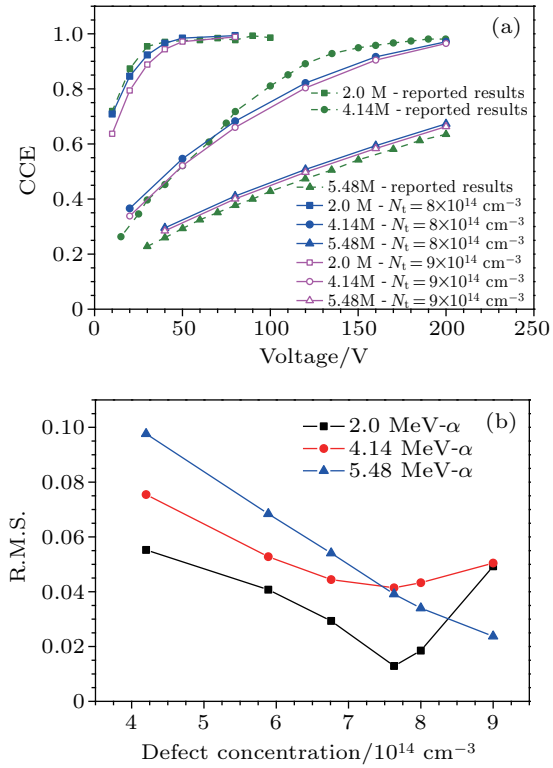


Fig. 7. Quantification of the similarity between simulation and experimental results. (a) CCE_{sim} with larger N_t compared with CCE_{exp}. (b) R.M.S calculated for α particle with various energies.

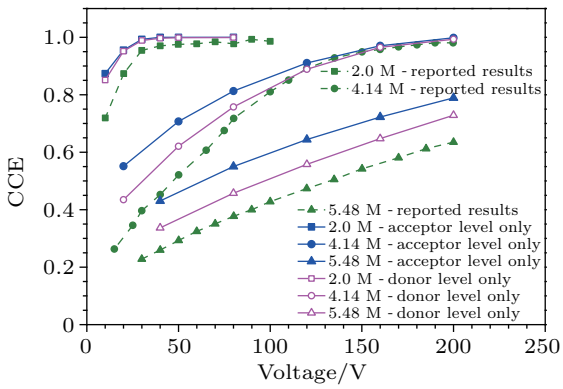


Fig. 8. CCE_{sim} calculated with acceptor/donor level only when $N_t = 7.63 \times 10^{14}$ cm^{-3}.

An N_t larger than 7.63×10^{14} cm^{-3} was also simulated (Fig. 7(a)) to find if there is a better alternative. Root-mean-square deviation (R.M.S) was calculated to compare the similarity between the simulation and experimental results (Fig. 7(b)). According to R.M.S, $N_t = 7.63 \times 10^{14}$ cm^{-3} could be the best value for our simulation.

In addition, CCE_{sim} was also calculated when only one defect level of $Z1/2$ was considered. N_t remains 7.63×10^{14} cm^{-3} for such simulation and the results are plotted in Fig. 8. CCE_{sim} are obviously larger than CCE_{exp}.

4.3. Electron irradiated detector

For electron irradiated detectors, a dose of 40 Mrad corresponds to $N_t = 7.63 \times 10^{14}$ cm^{-3}. Assuming a linear relationship between dose and N_t, then 0 rad corresponds to $N_t = 0$ and 20 Mrad corresponds to $N_t = 3.82 \times 10^{14}$ cm^{-3}.

CCE_{sim} for electron irradiation are shown in Fig. 9, in which three irradiation doses of 0 rad, 20 Mrad, and 40 Mrad are used in the simulation and CCE_{sim} for 0 rad matches CCE_{exp} very well which is set as a reference to find out a proper pair of τ_n and τ_p. With the same incidence particle of 4.14 MeV α, CCE_{sim} either for 20 Mrad or 40 Mrad shows a good agreement with CCE_{exp}. In the voltage range from 0 to 120 V, CCE_{sim} is slight larger than CCE_{exp} and in the voltage range from 120 to 200 V, CCE_{sim} is a little less than CCE_{exp}. Except for the reason mentioned in the above section, non-uniform doping in the epilayer might be another reason causing the difference between the calculation and experimental results.

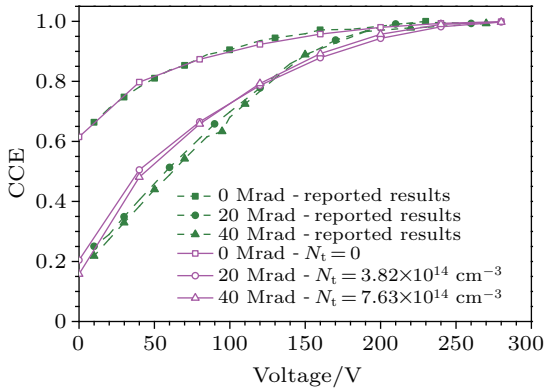


Fig. 9. Comparison between CCE_{sim} and CCE_{exp} for different electron irradiation doses.

4.4. ^{60}Co γ-ray irradiated detector

As 4H-SiC is classified as a highly radiation hard material for γ-ray,[3] the defect introduction rates of γ-ray to SiC epilayer are also less reported. Here, according to τ_p extracted in Ref. [9] for different cases of irradiation, N_t for 40 Mrad γ-ray was assumed in the range of 3.82×10^{13} cm^{-3} to 3.82×10^{14} cm^{-3}, and was finally determined to be 3.82×10^{14} cm^{-3}. CCE_{sim} against biased voltage is shown in Fig. 10.

For 40 Mrad, CCE_{sim} under an applied voltage lower than 80 V shows a good agreement with CCE_{exp}. But when the applied voltage is higher than 80 V, CCE_{sim} is smaller than

CCE_{exp}. For 20 Mrad, CCE_{sim} shows a good agreement with CCE_{exp} when the applied voltage is higher than 80 V, but is a bit larger than CCE_{exp} in the case of below 80 V.

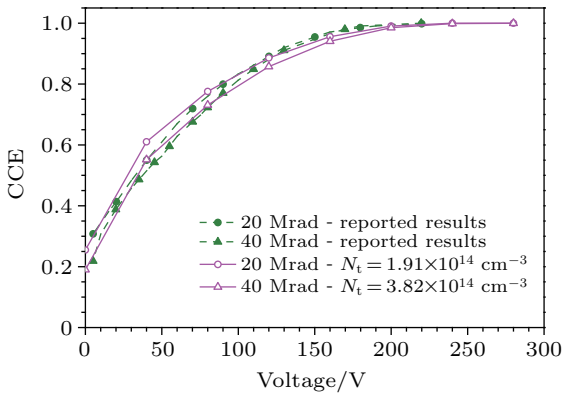


Fig. 10. Comparison between CCE_{sim} and CCE_{exp} for different γ irradiation doses.

5. Conclusion

The $Z1/2$ defect regarded as two individual defect levels was induced to investigate the degradation of SiC Schottky diode detector. Comparing the calculated CCE with experimental CCE, an acceptable approximation was achieved. It is believed that the $Z1/2$ defect could be treated as two independent defect levels in TCAD to simplify the simulation. It is feasible to analyze the performance of a detector if N_t and N_{eff} are given in spite of the incidence particle. The effect of other defects and the degradation of mobility should also be investigated if a more precise simulation is required. Based on such a treatment, our further work will focus on the investigation of numerical relationship between $Z1/2$ defect and carbon vacancy in SiC.[16]

References

[1] Hazdra P, ZaiHlava V and Vobecka J 2013 *Solid State Phenom.* **205-206** 451

[2] Quinn T, Bates R, Bruzzi M, Cunningham W, Mathieson K, Moll M, Nelson T, Nilsson H E, Pintillie I, Reynolds L, Sciortino S, Sellin P, Strachan H, Svensson B G, Vaitkus J and Rahman M 2004 *IEEE Nucl. Sci. Symp. Conf. Rec.*, 19–25 October 2003 OR Portland, p. 1028

[3] Nava F, Bertuccio G, Cavallini A and Vittone E 2008 *Meas. Sci. Technol.* **19** 102001

[4] Sciortino S, Hartjes F, Lagomarsino S, Nava F, Brianzi M, Cindro V, Lanzierif C, Mollg M and Vanni P 2005 *Nucl. Instrum. Methods Phys. Res. Sect. A* **552** 138

[5] Storasta L, Bergman J P, Janzen E, Henry A and Lu J 2004 *J. Appl. Phys.* **96** 4909

[6] Klein P B, Shanabrook B V, Huh S W, Polyakov A Y, Skowronski M, Sumakeris J J and O'Loughlin M J 2006 *Appl. Phys. Lett.* **88** 052110

[7] Klein P B 2008 *J. Appl. Phys.* **103** 033702

[8] Nigam S 2008 *Carrier Lifetimes in Silicon Carbide* (Ph. D. dissertation) (Pittsburgh: Carnegie Mellon University)

[9] Nava F, Vittone E, Vanni P, Verzellesi G, Fuochi P G, Lanzieri C and Glaser M 2003 *Nucl. Instrum. Methods Phys. Res. Sect. A* **505** 645

[10] Jaksic M, Bosnjak Z, Gracin D, Medunic Z, Pastuovic Z, Vittone E and Nava F 2002 *Nucl. Instrum. Methods Phys. Res. Sect. B* **188** 130

[11] Vittone E, Fizzotti F, Giudice A L, Paolini C and Manfredotti C 2000 *Nucl. Instrum. Methods Phys. Res. Sect. B* **161–163** 446

[12] Neamen and Donald A 2011 *Semiconductor Physics and Devices: Basic Principles* (3th Edn.) (Beijing: Publishing House of Electronic Industry) p. 156 (in Chinese)

[13] Castaldini A, Cavallini A, Rigutti L, Nava F, Ferrero S and Giorgis F 2005 *J. Appl. Phys.* **98** 053706

[14] Choo S C 1970 *Phys. Rev. B* **1** 687

[15] Synopsys Inc 2013 *Sentaurus Device User Guide* Ver. H-2013.03

[16] Klein P B 2009 *Phys. Status Solidi* **206** 2257

[17] Schenk A and Krumbein U 1995 *J. Appl. Phys.* **78** 3185

[18] Castaldini A, Cavallini A, Nava F, Fuochi P G and Vanni P 2003 *Mater. Sci. Forum* **433–436** 439

[19] Castaldini A, Cavallini A and Rigutti L 2006 *Semicond. Sci. Technol.* **21** 724

[20] Eberlein T A G, Jones R and Briddon P R 2003 *Phys. Rev. Lett.* **90** 225502

[21] Fageeha O, Howard J and Block R C 1994 *J. Appl.* **75** 2317

[22] Guo H Y, Ge C C, Xia M, Guo L P, Chen J H and Yan Z Q 2015 *Chin. Phys. B* **24** 037803

[23] Janzen E, Gali A, Carlsson P, Gallstrom A, Magnusson B and Son N T 2009 *Mater. Sci. Forum* **615–617** 347

[24] Jia R X, Zhang Y M and Zhang Y M 2010 *Chin. Phys. B* **19** 107105

[25] Kang S M, Ha J H, Park S H, Kim H S, Chun S D and Kim Y K 2007 *Nucl. Instrum. Methods Phys. Res.* **579** 145

[26] Moscatelli F 2007 *Nucl. Instrum. Methods Phys. Res. Sect. A* **583** 157

[27] Murat M, Akkerman A and Barak J 2009 *IEEE Trans. Nucl. Sci.* **55** 3046

[28] Omotoso E, Meyer W E, Rensburg P J J V, Igumbor E, Tunhuma S M, Ngoepe P N M, Danga H T and Auretet F D 2017 *Nucl. Instrum. Methods Phys. Res. B* **409** 241

[29] Raja P V and Murty N V L N 2018 *IIEEE Trans. Nucl. Sci.* **65** 558

[30] Strokan N B, Ivanov A M and Lebedev A A 2006 *Nucl. Instrum. Methods Phys. Res. Sect. A* **569** 758

[31] Vittone E, Pastuovic Z, Breese M B H, Garcia Lopez J, Jaksic M, Raisanen J, Siegele R, Simon A and Vizkelethy G 2016 *Nucl. Instrum. Methods Phys. Res. Sect. B* **372** 128

[32] Zh X and Hu X 2018 *Chin. Phys. B* **27** 087304

[33] Han Y, Li B S, Wang Z G, *et al.* 2017 *Chin. Phys. Lett.* **34** 012801

[34] Zhang L, Zhang Y M, Zhang Y M, Han Ch and Ma Y J 2009 *Chin. Phys. B* **18** 1931

[35] Zippelius B, Glas A, Weber H B, Pensl G, Kimoto T and Krieger M 2012 *Mater. Sci. Forum* **717–720** 251